Synthesis, Crystal Structure, and Optical and Magnetic Properties of a Novel Two-Dimensional Copper(II) Network Formed Conjointly with μ-Bipyrimidine, μ-Oxalato, and μ-Chloro Ligands[||]

Silvio Decurtins,*,[†] Helmut W. Schmalle,[†] Philippe Schneuwly,[†] Li-Min Zheng,[†] Jürgen Ensling,[‡] and Andreas Hauser[§]

Institut für Anorganische Chemie, Universität Zürich, Winterthurerstrasse 190, CH-8057 Zürich, Switzerland, Institut für Anorganische Chemie und Analytische Chemie, Johannes Gutenberg-Universität Mainz, Staudingerweg 9, D-55099 Mainz, Germany, and Institut für Anorganische und Physikalische Chemie, Universität Bern, Freiestrasse 3, CH-3009 Bern, Switzerland

Received April 14, 1995[⊗]

The preparation, X-ray crystal structure, and optical and magnetic properties of a polymeric two-dimensional μ-2,2′-bipyrimidine ($C_8H_6N_4$, bpym), μ-oxalato-bridged ($C_2O_4^{2-}$, ox) and μ-chloro-bridged copper(II) network of formula $[Cu_2(bpym)(ox)Cl_2]_n$ is reported. The compound crystallizes in the orthorhombic system, space group *Pbca*, with $a = 9.522(2)$ Å, $b = 10.509(2)$ Å, $c = 13.222(3)$ Å, $Z = 4$, and $V = 1323.1(5)$ Å^3. The structure consists of alternatingly μ-bpym- and μ-ox bridged copper(II) chains which again are connected through mono(μ-chloro) ligands, thus forming a corrugated two-dimensional (2D) framework. Polarized optical single crystal absorption spectra, measured at both room and liquid-helium temperatures, are presented and the absorption pattern is discussed using the selection rules derived from an orbital scheme of the Cu(II) chromophore with idealized C_{2v} symmetry. A low-lying MLCT state is taken as the origin of the strongly polarized absorption parallel to the *b*-axis, hence the ox−Cu(II)−bpym direction. The temperature dependence of the magnetic susceptibility is well explained with an alternating chain model, taking into account the strong intramolecular antiferromagnetic interaction through the μ-bpym and μ-ox bridges. The analysis is based on the Hamiltonian, $\hat{H} = -2J\sum_{i=1}^{n/2}[\hat{S}_{2i}\cdot\hat{S}_{2i-1} + \alpha\hat{S}_{2i}\cdot\hat{S}_{2i+1}]$, and the resulting exchange parameters are $J = -189(1)$ cm^{-1} for the μ-ox link and $\alpha J = -76(1)$ cm^{-1} for the μ-bpym link, which corresponds to an alternation parameter of $\alpha = 0.40(2)$. In addition, a mean-field correction is discussed which considers the possibility of weak "interchain" interactions mediated by the asymmetric mono(μ-chloro) bridges.

Introduction

The design of synthetic pathways to systems of desired properties continues to be a challenge for inorganic chemists. In this context, a great deal of interest has been devoted to the development of rational synthetic routes to novel one- to three-dimensional, polymeric coordination compounds which have applications as molecular-based magnetic materials.[1−3] Focusing on the approach of having transition metals as spin carrier centers, it is the declared target to optimize the number of chemical links between the magnetic ions in order to gain an increased contribution from intramolecular interactions and, at the same time, to diminish the influence of the weaker intermolecular contacts.

Along this line, many recent reports have focused on the synthesis and structural characterization of polymeric transition metal compounds using oxalate[4−8] or 2,2′-bipyrimidine[9−13] as chelating and bridging ligand systems. The striking structural similarity between these two bridging units suggests synthetic experiments aimed at combining both ligands in order to design extended networks. This goal has successfully been realized with the synthesis of a bridged copper(II) compound with alternating bipyrimidine and oxalate ligands, thus forming a honeycombed layered structure[10] similar to the purely oxalato bridged two-dimensional network.[7] So far, the selection of the structural possibilities resulting from a combination of these comparable bridging ligands has not yet been exhausted. By making use of the known plasticity of the coordination sphere of copper(II), configurations other than the tris-chelated form can be designed. By offering a further potentially bridging ligand in the form of Cl^- ions, in addition to bpym and oxalate,

[†] Universität Zürich.
[‡] Johannes Gutenberg-Universität Mainz.
[§] Universität Bern.
[||] Dedicated to Professor Philipp Gütlich on the occasion of his 60th birthday.
[⊗] Abstract published in *Advance ACS Abstracts,* October 1, 1995.

(1) *Magnetic Molecular Materials*; Gatteschi, D., Kahn, O., Miller, J. S., Palacio, F., Eds.; Kluwer Academic Publishers: Dordrecht, The Netherlands, 1991.
(2) *Proceedings of the International Symposium on Chemistry and Physics of Molecular Based Magnetic Materials;* Iwamura, H., Itoh, K., Kinoshita, M., Eds.; Molecular Crystals and Liquid Crystals; Gordon & Breach: London, 1993.
(3) *Proceedings of the IV International Conference on Molecule-Based Magnets*; Miller, J. S., Epstein, A. J., Eds.; Molecular Crystals and Liquid Crystals; Gordon & Breach: London, 1995.
(4) Tamaki, H.; Zhong, Z. J.; Matsumoto, N.; Kida, S.; Koikawa, M.; Achiwa, N.; Hashimoto, Y.; Okawa, H. *J. Am. Chem. Soc.* **1992**, *114*, 6974.
(5) Atovmyran, L. O.; Shilov, G. V.; Lyubovskaya, R. N.; Zhilyacva, E. I.; Ovanesyan, N. S.; Pirumova, S. I.; Gusakovskaya, I. G. *JETP Lett.* **1993**, *58*, 766.
(6) Decurtins, S.; Schmalle, H. W.; Schneuwly, P.; Oswald, H. R. *Inorg. Chem.* **1993**, *32*, 1888.
(7) Decurtins, S.; Schmalle, H. W.; Oswald, H. R.; Linden, A.; Ensling, J.; Gütlich, P.; Hauser, A. *Inorg. Chim. Acta* **1994**, *216*, 65.
(8) Decurtins, S.; Schmalle, H. W.; Schneuwly, P.; Ensling, J.; Gütlich, P. *J. Am. Chem. Soc.* **1994**, *116*, 9521.
(9) Julve, M.; De Munno, G.; Bruno, G.; Verdaguer, M. *Inorg. Chem.* **1988**, *27*, 3160.
(10) De Munno, G.; Julve, M.; Nicolo, F.; Lloret, F.; Faus, J.; Ruiz, R.; Sinn, E. *Angew. Chem.* **1993**, *105*, 588.
(11) De Munno, G.; Julve, M.; Lloret, F.; Faus, J.; Verdaguer, M.; Caneschi, A. *Angew. Chem.* **1993**, *105*, 1122.
(12) De Munno, G.; Bazzicalupi, C.; Faus, J.; Lloret, F.; Julve, M. *J. Chem. Soc., Dalton Trans.* **1994**, 1879.
(13) De Munno, G.; Julve, M.; Lloret, F.; Faus, J.; Verdaguer, M.; Caneschi, A. *Inorg. Chem.* **1995**, 34, 157.

0020-1669/95/1334-5501$09.00/0

a new two-dimensional copper(II) network consisting of μ-bpym, μ-ox, and μ-Cl bonds has been realized.

We report here the preparation, crystal structure, and single crystal optical absorption spectra of the title compound. The description of the magnetic properties is based on an alternating-chain model, combined with a mean-field correction, which accounts for the two-dimensional character of the structure.

Experimental Section

Materials. All reagents were commercial grade materials, used as received. 2,2′-Bipyrimidine was purchased from Johnson Matthey. $K_3[Cr(ox)_3]\cdot 3H_2O$ was prepared according to the literature method.[14]

Preparation of Microcrystalline $[Cu_2(bpym)(ox)Cl_2]_n$. An aqueous solution containing stoichiometric amounts of $CuCl_2\cdot 2H_2O$ (0.05 M) and 2,2′-bipyrimidine was mixed with a stoichiometric aqueous solution of oxalic acid. Instantaneously, a green microcrystalline precipitate started to appear; it was filtered off, washed with water, and dried in air. The X-ray powder diffraction data showed it to be structurally isomorphous to the single crystals which have been prepared as described below.

Preparation of Single Crystals of $[Cu_2(bpym)(ox)Cl_2]_n$. In order to favor single crystal growth, the educt concentrations had to be decreased and oxalic acid was replaced by the complex $[Cr(ox)_3]^{3-}$ anion which acts as a source of the oxalate ion at a slow rate. An aqueous solution containing stoichiometric amounts of $CuCl_2\cdot 2H_2O$ (0.01 M) and 2,2′-bipyrimidine was mixed with a 0.002 M aqueous solution of $K_3[Cr(ox)_3]\cdot 3H_2O$. Slow evaporation of this solution yielded prismatic-shaped, green single crystals. Anal. Calcd for $[Cu_2(bpym)(ox)Cl_2]$: C, 27.04; H, 1.36; N, 12.61; Cl, 15.96; Cu, 28.61. Found: C, 27.10; H, 1.45; N, 12.85; Cl, 15.75; Cu, 28.65.

Crystallographic Structure Determination. A total of 4263 intensity data (including 54 standards) were collected on an Enraf-Nonius CAD-4 four-circle diffractometer, using graphite-monochromated Mo Kα radiation (λ = 0.710 73 Å). The unit cell parameters and the orientation matrix were determined by a standard least-squares refinement (Enraf-Nonius CAD-4 software[15]) of the setting angles of 25 automatically centered reflections in the range $4.9° < \theta < 24.0°$. The stability of the crystal was checked every 3 h by measuring three standard reflections; no loss of intensity was noted. To control the orientation of the crystal, three standard reflections were remeasured every 400 reflections during the data collection, which was performed by the $\omega-2\theta$ scan technique in a zigzag mode. The data were corrected for Lorentz and polarization effects. A face-indexed (seven crystal faces) numerical absorption correction was applied. The crystal volume was 0.015 mm^3.

The structure was solved using the Patterson interpretation routine of SHELXS-86[16] and refined by full matrix least squares calculations on F_{hkl}^2 with SHELXL-93[17] which was also used for the final geometrical calculations. Hydrogen atoms were refined with isotropic displacement parameters. Further crystallographic data and details of the refinement are summarized in Table 1. The largest and mean Δ/σ are 0.001 and 0.000. In the final difference electron density map the residual maxima and minima were +0.61 and −0.65 e Å^{-3}. Final positional parameters (including H-atoms) of the title compound are listed in Table 2. A list of interatomic bond distances and angles are given in Table 3. Anisotropic displacement parameters (Table S2) are available as supplementary material.

Optical Measurements. Polarized single crystal absorption spectra of $[Cu_2(bpym)(ox)Cl_2]_n$ with the *E*-vector parallel and perpendicular to the crystal *b*-axis were recorded on a Cary 5e spectrometer using a pair of matched Glan-Taylor polarizers. A crystal of dimensions $\approx 0.3 \times 0.1 \times 0.1$ mm^3 was mounted on a piece of copper foil having a suitable aperture. The copper foil, in turn, was inserted into an Air Products closed cycle cryostat achieving temperatures down to 12 K.

Table 1. Crystal Data for $[Cu_2(bpym)(ox)Cl_2]_n$

formula	$C_{10}H_6N_4O_4Cl_2Cu_2$
fw	444.16
temp,K	295(2)
space group	*Pbca* (No. 61)
a, Å	9.522(2)
b, Å	10.509(2)
c, Å	13.222(3)
V, Å^3	1323.1(5)
Z	4
d_{calcd}, g cm^{-3}	2.230
d_{obsd}, g cm^{-3}	2.20
λ(Mo Kα), Å	0.710 73
μ, cm^{-1}	3.641
R^a	0.0313
$R_w{}^a$	0.0820

^{a} $R = \sum||F_o| - |F_c||/\sum|F_o|$. $R_w = [\sum w(F_o^2 - F_c^2)^2/\sum w(F_o^2)^2]^{1/2}$.

Table 2. Positional and Equivalent Isotropic Displacement Parameters for $[Cu_2(bpym)(ox)Cl_2]_n$

atom	*x/a*	*y/b*	*z/c*	U_{eq},^{a} Å^2
Cu	0.5243(1)	0.2432(1)	−0.0073(1)	0.027(1)
Cl	0.2632(1)	0.2558(1)	0.0957(1)	0.033(1)
C(11)	0.4613(3)	0.0008(2)	−0.0526(2)	0.018(1)
O(11)	0.4452(2)	0.1069(2)	−0.0933(2)	0.024(1)
O(21)	0.5756(2)	0.1047(2)	0.0866(2)	0.025(1)
N(1)	0.4537(3)	0.3874(2)	−0.0947(2)	0.021(1)
C(2)	0.4658(3)	0.4997(2)	−0.0507(2)	0.018(1)
N(3)	0.4278(3)	0.6115(2)	−0.0876(2)	0.020(1)
C(4)	0.3697(3)	0.6105(3)	−0.1792(2)	0.027(1)
C(5)	0.3498(4)	0.4982(3)	−0.2320(2)	0.024(1)
C(6)	0.3956(4)	0.3866(3)	−0.1870(2)	0.026(1)
H(4)	0.338(3)	0.687(3)	−0.209(2)	0.020(7)
H(5)	0.300(4)	0.497(3)	−0.292(2)	0.023(8)
H(6)	0.383(3)	0.311(3)	−0.219(2)	0.014(7)

^{a} $U_{eq} = {}^1/_3\sum_i\sum_j U_{ij}a_i^*a_j^*\mathbf{a}_i\cdot\mathbf{a}_j$.

Table 3. Selected Bond Distances (Å) and Angles (deg)^a for $[Cu_2(bpym)(ox)Cl_2]_n$

Cu−Cl	2.838(1)	Cu−N(3)^i	2.027(2)
Cu−Cl^{iii}	2.557(1)	C(11)−O(21)^{ii}	1.247(3)
Cu−O(11)	1.978(2)	C(11)−O(11)	1.247(3)
Cu−O(21)	1.975(2)	C(11)−C(11)^{ii}	1.574(5)
Cu−N(1)	2.020(2)		
O(21)−Cu−O(11)	85.5(1)	N(3)^i−Cu−Cl	82.3(1)
O(21)−Cu−N(1)	174.1(1)	N(3)^i−Cu−Cl^{iii}	94.6(1)
O(21)−Cu−N(3)^i	96.4(1)	Cl−Cu−Cl^{iii}	176.7(1)
O(21)−Cu−Cl	87.1(1)	O(21)^{ii}−C(11)−O(11)	127.2(2)
O(21)−Cu−Cl^{iii}	94.0(1)	O(21)^{ii}−C(11)−C(11)^{ii}	116.1(2)
O(11)−Cu−N(1)	95.1(1)	O(11)−C(11)−C(11)^{ii}	116.7(2)
O(11)−Cu−N(3)^i	170.6(1)	C(11)−O(11)−Cu	110.7(2)
O(11)−Cu−Cl	88.6(1)	C(11)^{ii}−O(21)−Cu	111.1(2)
O(11)−Cu−Cl^{iii}	94.5(1)	C(2)−N(1)−Cu	112.9(2)
N(1)−Cu−N(3)^i	82.2(1)	C(6)−N(1)−Cu	130.8(2)
N(1)−Cu−Cl	87.0(1)	C(2)−N(3)−Cu^i	112.3(2)
N(1)−Cu−Cl^{iii}	91.8(1)	C(4)−N(3)−Cu^i	131.5(2)

^{a} Symmetry code: (i) $1-x, 1-y, -z$; (ii) $1-x, -y, -z$; (iii) $^1/_2+x, {}^1/_2-y, -z$.

Magnetic Measurements. Magnetic susceptibility data were collected with a vibrating sample magnetometer (Princeton Applied Research) which was calibrated with $Hg[Co(NCS)_4]$; the system was equipped with a combined He−bath-continuous-flow cryostat (Cryovac) and allowed measurements in the temperature range of 2−295 K. Susceptibility data between ambient temperature and 400 K were obtained by using a SQUID magnetometer (MPMS, Quantum Design Instruments). Both magnetometers were operated at a magnetic field of 1 T. The powdered sample (35 mg) was contained in a quartz tube. The magnetometer output was corrected for the diamagnetism of the holder and the underlying diamagnetism of the constituent atoms on the basis of Pascal's constants (χ_{dia}: -214×10^{-6} cm^3 mol^{-1}). A value of 60×10^{-6} cm^3 mol^{-1} per Cu atom was assumed for the temperature independent paramagnetism (TIP).

ESR Measurements. The ESR measurements were made with a

(14) Bailar, J. C.; Jones, E. M. In *Inorganic Syntheses*; Booth, H. S., Ed.; McGraw-Hill Book Co.: New York, 1939; Vol. 1, p 35.
(15) Enraf-Nonius CAD-4 Software,Version 5.0, Enraf-Nonius, Delft, The Netherlands, 1989.
(16) Sheldrick, G. M. SHELXS-86, Crystal Structure Solution. In *Crystallographic Computing*; Sheldrick, G. M., Krüger, C., Goddard, R., Eds.; Oxford University Press: Oxford, England, 1985; p 175.
(17) Sheldrick, G. M. *J. Appl. Crystallogr.*, manuscript in preparation.

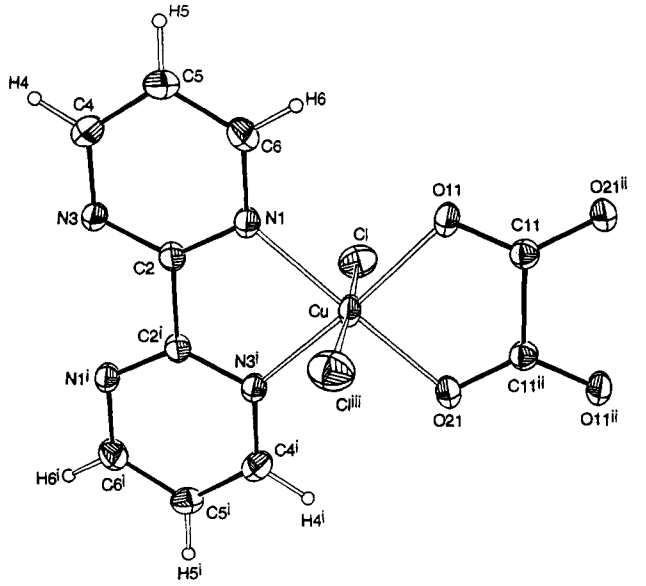

Figure 1. ORTEP plot (50% probability level) of the copper(II) chromophore in $[Cu_2(bpym)(ox)Cl_2]_n$.

Bruker ESP 300 spectrometer at X-band frequency between ambient temperature and 130 K.

Results and Discussion

Description of the Structure of $[Cu_2(bpym)(ox)Cl_2]_n$. The structure of the compound is made up of a two-dimensionally linked copper(II) network with an alternating, bis-chelating μ-bpym and μ-ox coordination along one direction (parallel to the crystallographic *b*-axis) and an asymmetric mono(μ-chloro) bridge in the perpendicular direction (along the crystallographic *a*-axis). The copper atom of the $CuN_2O_2Cl_2$ chromophore shows a 2 + 2 + 1 + 1 coordination, whereby the four equatorial positions are occupied by two nitrogen atoms of bpym and two oxygen atoms of oxalate and the axial sites are asymmetrically filled by two chloride atoms. A perspective view of the copper environment, with the atom-numbering scheme, is depicted in Figure 1. The four equatorial atoms are nearly coplanar with deviations from the least-squares plane being less than 0.029(1) Å, the copper atom being displaced 0.130(1) Å toward the nearer chloride atom (Cl^{iii}).

The Cu−O bond lengths are slightly larger compared with the values of a chelating, but nonbridging Cu−oxalate complex [mean value: 1.935(6) Å][12] but they are significantly shorter than in the layered $[Cu_2(bpym)(ox)_2]\cdot H_2O$ compound [mean values: equatorial 2.086(3); axial 2.076(3) Å].[12] The carbon−carbon and carbon−oxygen bonds of the planar oxalate ligand (C(11) and $C(11)^{ii}$ are related by a center of symmetry; see Table 3) compare well with those from another bis-chelating μ-ox bridged compound.[7]

The Cu−N bond distances are only slightly shorter than those reported for a similar Cu(II)-bpym-Cu(II) unit [Cu−N: mean value 2.045(5) Å].[11] The carbon-carbon and carbon-nitrogen bonds of the bridging bpym group compare well with those found for other coordinated bpym ligands.[18] The pyrimidyl rings of bpym show only small deviations from planarity [largest deviation is 0.009(2) Å for C(5)], and they are mutually related through an inversion symmetry operation.

The chloride atoms on the axial positions show two distinctly different and rather long bond lengths. On one side, both are definitely longer than the Cu(II)−Cl distance of 2.252(1) Å found in the equatorial plane of $[Cu_2(bpym)Cl_4]$.[9] On the other side, the value of 2.869(1) Å for the axial Cu(II)−Cl distance of the referred compound compares well with the longer Cu−Cl bond length determined in the title complex. These bond distances may also be compared with the values determined in a zigzag mono(μ-chloro) Cu(II) chain structure with alternating short ($average_{basal}$: 2.276 Å) and long ($average_{apical}$: 2.830 Å) Cu−Cl distances.[19]

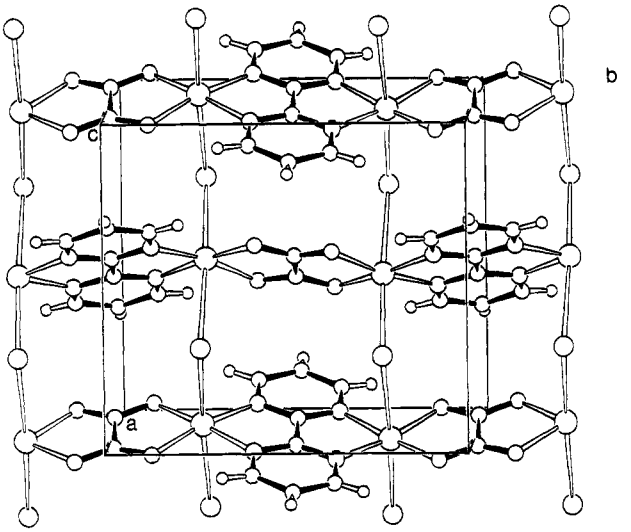

Figure 2. View, approximately along the *c*-axis, exhibiting only one layer of the structure.[28]

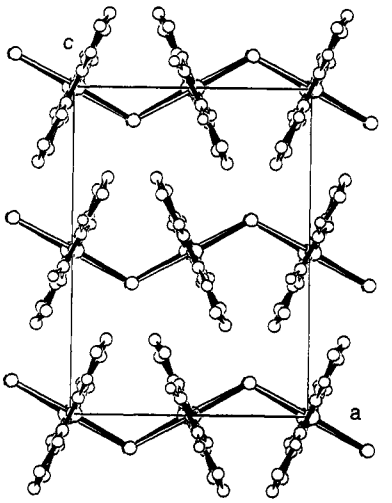

Figure 3. A [010] projection of $[Cu_2(bpym)(ox)Cl_2]_n$, accentuating the corrugated form of the polymeric layer compound.

Figure 2, roughly a [001] projection, clearly demonstrates the polymeric two-dimensional character of the structure. This view also draws special attention to the fact that adjacent chains parallel to the *b*-axis regularly alternate in the sequence of the two bis-chelating bridging ligands, whereby the μ-chloro ligands connect adjacent chains along the *a*-axis. There are two intrachain Cu···Cu separations, namely 5.420(1) Å for Cu−bpym−Cu and 5.137(1) Å for Cu−ox−Cu. These very similar values finally lead to the regular structural feature of the compound. The shortest intramolecular Cu···Cu separation along the *a*-axis is 4.767(1) Å. The shortest interlayer Cu···Cu distance is 6.613(2) Å. In Figure 3, a [010] projection, the corrugated form of the polymeric layers is accentuated. The two independent Cu−Cl−Cu bridging angles are 124.1(1)° and 124.8(1)°. Finally, Figure 4 shows a stereoview of the packing arrangement of the title compound.

(18) De Munno, G.; Bruno, G.; Nicolo, F.; Julve, M.; Real, J. A. *Acta Crystallogr.* **1993**, *C49*, 457.

(19) Cortés, R.; Lezama, L.; Ruiz de Larramendi, J. I.; Madariaga, G.; Mesa, J. L.; Zuniga, F. J.; Rojo, T. *Inorg. Chem.* **1995**, *34*, 778.

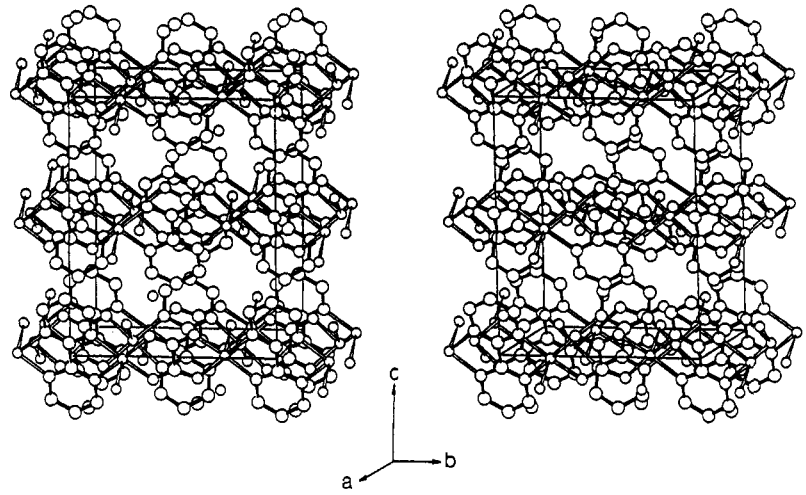

Figure 4. Stereoview of the layered packing of $[Cu_2(bpym)(ox)Cl_2]_n$.

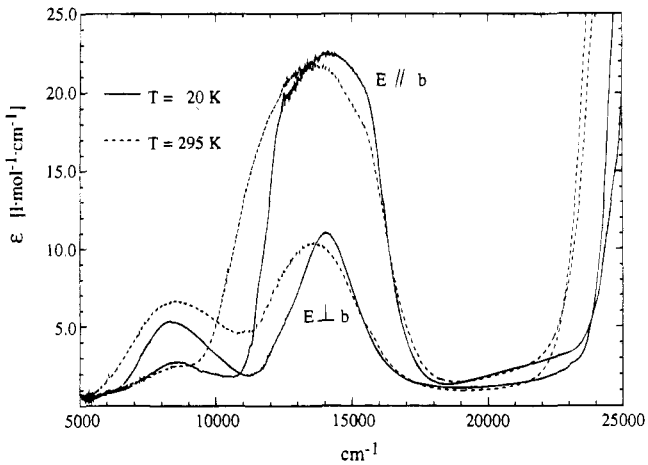

Figure 5. Polarized single crystal absorption spectra of $[Cu_2(bpym)(ox)Cl_2]_n$ at 293 and 20 K with E parallel and perpendicular to the crystal b-axis.

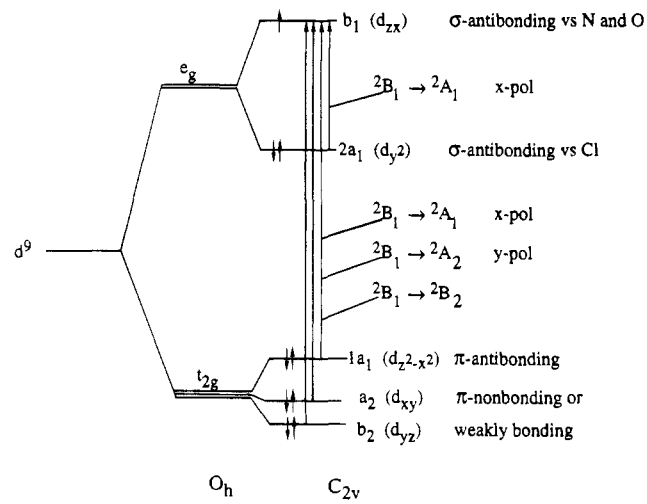

Figure 6. Splitting of the d-orbitals for $[Cu_2(bpym)(ox)Cl_2]_n$ in idealized C_{2v} symmetry, and selection rules for the resulting d−d transitions. The actual site symmetry is C_s, and the above selection rules are relaxed.

Optical Properties. Figure 5 shows the polarized absorption spectra in the near IR and visible energy range of $[Cu_2(bpym)(ox)Cl_2]_n$ at 295 and 20 K with the E-vector parallel and perpendicular to the crystal b-axis. There are two prominent bands, one centered at 8400 cm^{-1} and strongly polarized perpendicular to the b-axis, the other one centered at 14 000 cm^{-1} and predominantly polarized parallel to the b-axis. The latter obviously consists of more than one component having intensities both with E parallel and perpendicular to b. With molar extinction coefficients of ≈5−30 L/mol·cm all these bands are spin-allowed d−d bands. Above 23 000 cm^{-1}, intense MLCT bands set in.

The observed absorption spectra in the region of the d−d transitions can be rationalised on the basis of the orbital diagram shown in Figure 6. The orbitals and the states resulting from the d^9 electron configuration of Cu(II) are labelled according to an idealised C_{2v} geometry, with the bisecting angle of the chelate ligands as the molecular z-axis, and the Cu−Cl direction as the y-axis. Thus, the d_{zx} (b_1) orbital is the most σ-antibonding orbital as it has lobes extended in the direction of the N and O atoms of the chelate ligands. The d_{y^2} ($2a_1$) orbital is σ-antibonding toward the Cl^- ions. It is substantially lower in energy than the d_{zx} orbital, because (i) Cl^- is much lower in the spectrochemical series, and (ii) both nonequivalent Cu−Cl bond lengths are long compared with bond distances found for equatorially coordinated chloride ions.[19] The exact order of the π-orbitals, d_{xy} (a_2), d_{yz} (b_2), and $d_{z^2-x^2}$ ($1a_1$) is not quite as straightforward. Their relative energies depend critically upon the π-donor and π^*-acceptor properties of the ligands. Whereas the π-interaction with the Cl^- ions is negligible, the negatively charged oxalate ions act as π-donors both parallel and perpendicular to the ligand plane,[20] and bpym with its comparatively low-lying π^*-orbitals is a potential π^*-acceptor with regard to the π-interaction perpendicular to the ligand plane.[21] Bearing this in mind, we believe the $d_{z^2-x^2}$ orbital is in all probability the highest energy π-orbital because of the antibonding π-interaction parallel to the ligand planes of both oxalate and bpym. The lowest energy d-orbitals then are the d_{xy} and the d_{yz} orbitals, which are more or less nonbonding, since the π-donor interaction of the oxalate counteracts the π^*-acceptor interaction of the bpym perpendicular to the ligand planes. With idealized bite angles of 90° for the two chelate ligands, these two orbitals would be degenerate. However, taking into account the actual bite angles, this degeneracy is lifted. Depending upon whether the π^*-acceptor properties of bpym or the π-donor properties of oxalate are dominant, either the d_{yz} or the d_{xy} orbital is the lowest energy d-orbital.

How does this relate to the experimental spectra? With Cu(II) having a d^9 electron configuration, the electronic ground state is a $^2B_1$ state, i.e. with a hole in the b_1 orbital. The lowest excited state, corresponding to a promotion of an electron from

(20) (a) Atanasov, M. A.; Schönherr, T.; Schmidtke, H. H. *Theor. Chim. Acta* **1987**, *71*, 59. (b) Atanasov, M. A.; Schönherr, T. *Inorg. Chem.* **1990**, *29*, 4545.

(21) Schönherr, T.; Degen, J. *Z. Naturforsch.* **1990**, *45A*, 161.

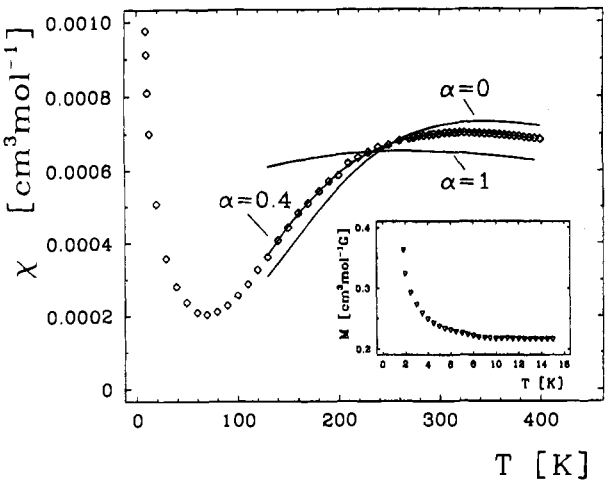

Figure 7. Magnetic susceptibility data for $[Cu_2(bpym)(ox)Cl_2]_n$. The fitted curve describing the data between 130−400 K was calculated from an alternating-chain model with $S = {}^1/_2$. The failure of the uniform-chain ($\alpha = 1$) and the dimer ($\alpha = 0$) model to fit the experimental data is obvious. The inset displays the field-cooled magnetization in the low-temperature range.

the $2a_1$ orbital to the b_1 orbital, is a $^2A_1$ state. According to electric-dipole selection rules (there is no inversion center present at the Cu site) the $^2B_1 \rightarrow {}^2A_1$ transition is polarized with the electric field vector E along the molecular x-axis. The molecular x-axis, in turn, is approximately perpendicular to the crystal b-axis. Thus the band in the near IR can be assigned to the $^2B_1 \rightarrow {}^2A_1$ transition, the comparatively high energy of the transition being due to the very different σ-donor properties of the Cl^- ligand on the one hand and of the oxalate and bpym ligands on the other. The various components of the band in the visible region thus have to be assigned to transitions arising from the promotion of an electron from the π-orbitals to the b_1 orbital. In C_{2v}, the corresponding transitions $^2B_1 \rightarrow {}^2A_1$, $^2B_1 \rightarrow {}^2A_2$, and $^2B_1 \rightarrow {}^2B_2$ are x- and y-polarized and electric-dipole forbidden, respectively. There is no transition expected with z-polarization, this means with $E \parallel b$. However, since the local symmetry is lower than C_{2v}, this selection rule is certainly relaxed. Nevertheless, at a first glance it is still surprising that the $E \parallel b$ band is the most intense of all the bands in the region of the d−d transitions. Since d−d transitions get their intensities through mixing with CT states, the nature of the lowest energy CT state is crucial. In the case of the $[Cu(bpym)(ox)Cl_2]^{2-}$ entities, this is most certainly a MLCT state corresponding to the transfer of an electron from the metal to π^*-orbitals on bpym. Such an MLCT transition would, of course, be polarized along the Cu-bpym direction, which corresponds with the crystal b-axis. Thus, any d−d transition which gets its intensity through mixing with this low-lying MLCT state as a result of the effective low symmetry is polarized along the b-axis too.

To sum up, the orbital scheme of Figure 6 gives a good qualitative description of the bonding and spectroscopic properties of this interesting kind of Cu(II) chromophore. It may be corroborated by angular overlap type calculations using reasonable values for the angular overlap parameters e_σ and $e_{\pi(\text{parallel})}$ and $e_{\pi(\text{perpendicular})}$.[20,21] More sophisticated calculations, such as extended Hückel calculations, are not necessary at this stage.

Magnetic Properties. The magnetic susceptibility per Cu atom of a powdered sample of $[Cu_2(bpym)(ox)Cl_2]_n$ is shown in Figure 7 in the form of a χ vs T plot. The susceptibility exhibits a broad rounded maximum at about 320 K, followed by a minimum near 65 K. Below that temperature, the susceptibility curve increases with decreasing temperature. The low-temperature data (15−50 K) were fitted to a Curie−Weiss law, $\chi = C/(T - \Theta)$ and are thought to arise mainly from a small portion (≤2%) of paramagnetic impurities. The broad maximum in the curve in the high temperature range is characteristic for a large antiferromagnetic coupling between the copper complexes. From the known magnetostructural data for bpym- and ox-bridged copper(II) complexes, a predominantly antiferromagnetic exchange interaction along the pathway of the alternatingly bridged μ-bpym, μ-ox chains of the polymeric compound could be expected. Consequently, the data were analyzed first by use of an analytical expression for the exchange coupling in an alternating chain of $S = {}^1/_2$ ions developed by Hall[22] which has the following form:

$$\chi = \frac{Ng^2\mu_B^2}{kT}F(J,T) \tag{1}$$

$$F(J,T) = \frac{A + Bx + Cx^2}{1 + Dx + Ex^2 + Fx^3} \tag{2}$$

with $x = |J|/kT$ and N, μ_B, g, and k have their usual meanings. The coefficients $A-F$ are functions of the alternation parameter α defined by the Hamiltonian

$$\hat{H} = -2J\sum_{i=1}^{n/2}[\hat{S}_{2i}\cdot\hat{S}_{2i-1} + \alpha\hat{S}_{2i}\cdot\hat{S}_{2i+1}] \tag{3}$$

where J is the exchange coupling parameter associated with a particular copper(II) pair and αJ is the exchange constant associated with the adjacent unit. With this expression, the "best fit" (Figure 7) for the susceptibility after correcting for the above-described Curie−Weiss behavior of the paramagnetic species resulted in $J = -189(1)$ cm^{-1}, $g = 2.21(2)$ and the alternation parameter $\alpha = 0.40(2)$. The calculation was limited to the data points between 130 and 400 K, since below $kT/|J| = 0.5$ the theoretical results are not reliable.[22] Taking for granted that oxalate is responsible for the higher exchange coupling constant, $J = -189(1)$ cm^{-1}, accordingly the value of $\alpha J = -76(1)$ cm^{-1} corresponds to the exchange parameter for the bpym ligand.[9]

Both bridging ligand systems correspond well with the results from analogous binuclear or polymeric Cu(II) complexes. The singlet−triplet energy gap ($2J$) arising from the intramolecular interaction within a dimeric antiferromagnetically μ-ox-bridged Cu(II) complex of equivalent geometry has been determined to be -385.4 cm^{-1}.[23] For a recently reported series of one-dimensional compounds containing the Cu−bpym−Cu units, the antiferromagnetic coupling parameters ($2J$) were determined with values in the range of -135 cm^{-1} to -145 cm^{-1}.[24]

The influence of α on the magnetic curve is illustrated in Figure 7, with the fitted curves corresponding with the behavior of a dimer ($\alpha = 0$, $J = -190$ cm^{-1}) and a uniform chain ($\alpha = 1$, $J = -160$ cm^{-1}). The inability of these models to describe the experimental data is obvious.

In addition, the ESR spectra of the polycrystalline sample measured at X-band frequency between ambient temperature and 130 K revealed broad signals, however they clearly display features of axial symmetry with $g_\parallel = 2.29$ and $g = 2.07$.

Although the experimental data are described perfectly by the model for an alternating chain of $S = {}^1/_2$ ions with very reasonable exchange parameters, the two-dimensional character of the structure, that is the "interchain" interaction through the

(22) Hall, J. W.; Marsh, W. E.; Weller, R. R.; Hatfield, W. E. *Inorg. Chem.* **1981**, *20*, 1033.
(23) Julve, M.; Verdaguer, M.; Charlot, M.-F.; Kahn, O. *Inorg. Chim. Acta* **1984**, *82*, 5.
(24) De Munno, G.; Julve, M.; Lloret, F.; Faus, J.; Verdaguer, M.; Caneschi, A. *Inorg. Chem.* **1995**, *34*, 157.

axially positioned chloride ions, should also be examined. This problem was treated with a molecular-field correction which was inserted into expression 1 giving eq 4,[25] where χ_{Cu} is the

$$\chi_{Cu} = \frac{Ng^2\mu^2_B F(J,T)}{[kT - 2zJ'F(J,T)]} \quad (4)$$

susceptibility per Cu ion, z is the number of nearest neighbors in adjacent chains, and J' is the "interchain" exchange parameter. Each copper ion has two chloro-bridged nearest neighbors within the layered structure; thus, z was taken to be 2. This expression, including the Curie–Weiss behavior of the paramagnetic impurity, was fitted to the experimental magnetic susceptibility data by using the minimum of the factor R defined as $R = \sum_i (\chi_i^{calcd} - \chi_i^{obsd})^2/\sum_i(\chi_i^{obsd})^2$ as the criterion of the "best fit". The parameters obtained were $J = -189(1)$ cm^{-1}, $g = 2.17(2)$, $\alpha = 0.40(2)$, and $J' = +16(2)$ cm^{-1}.

The relatively large value of this additional exchange parameter (J'), resulting from the mean-field model, could be subject to question. The ligand configuration of the copper complex is by far not favorable for an "interchain" exchange interaction, since the magnetic orbital points from the copper atom toward the two oxygen and the two nitrogen atoms in the equatorial plane. It is favorably oriented to give a strong σ in-plane overlap and hence a strong antiferromagnetic interaction within the μ-bpym, μ-ox chains. The chloride ions bridge the copper atoms in loosly bonded axial positions (defined as the molecular y-axis), where the spin density of the unpaired electron is expected to be very low. Only a small admixture of the magnetic orbital d_{zx} with the d_y2 orbital, due to deviations from idealized single-ion C_{2v} symmetry, could be expected.

The structural feature of symmetrical and asymmetrical Cu–Cl-Cu linkages is well documented for many chain compounds.[26] There are predominately examples of linear chains exhibiting antiferromagnetic exchange coupling, and only very few ferromagnetic compounds have been observed. As an example, [Cu(DMSO)Cl$_2$] reveals an intrachain parameter $J = +31(4)$ cm^{-1}, whereby it has to be noted that the bridging geometry is quite different from that for the compound in the present report.[27] In any event, since small changes in the coordination geometry are associated with profund changes in the exchange to the point where even the sign of the exchange will be reversed, no final conclusions could be drawn from literature values based on different geometric environments.

Additionally, there is a sharp deviation of the data at temperatures ≤ 8 K from the Curie–Weiss law of the paramagnetic species in the sample. This may be due to a 3D ordering of the system at very low temperatures. A field-cooled magnetization (FCM) experiment in the low temperature range ($H = 50$ G; $2 \leq T \leq 15$ K) corroborates this assumption; the FCM curve (see inset in Figure 7) shows the typical feature of a ferromagnetic transition, i.e. a rapid increase of the magnetization M when T decreases; in this case only the onset of the transition can be detected at the lowest temperature of our instrument.

Concluding Remarks

The results described in the present paper show that an extended two-dimensional Cu(II) complex can be built up from μ-bipyrimidine, μ-oxalato, and μ-chloro ligands. The regular structure is a consequence of the very similar bridging geometry of the μ-bpym and μ-ox ligands. Both bridging units, alternatingly arranged along one direction, mediate a strong σ in-plane antiferromagnetic interaction between the copper atoms. Thus, an alternating chain model was successfully applied, whereby very reasonable exchange parameters resulted.

Acknowledgment. Gratitude is expressed to the Swiss National Science Foundation for financial support under Project No. 21-39250.93 / 21-33184.92 and to Professor H. R. Oswald for continous support of this project. The authors also thank Dr. Th. Schönherr, University of Düsseldorf, for his advice regarding AOM calculations, Dr. J. Pebler, University of Marburg, for performing the magnetic measurements in the high-temperature range and Dr. A. Linden, University of Zürich, for helpfully reading the manuscript.

Supporting Information Available: Tables of crystal data and data collection parameters (Table S1), anisotropic displacement parameters (Table S2), and complete bond distances and angles (Table S3) (3 pages). Ordering information is given on any current masthead page.

IC950443H

(25) Ginsberg, A. P.; Lines, M. E. *Inorg. Chem.* **1972**, *11*, 2289.
(26) Hatfield, W. E.; Estes, W. E.; Marsh, W. E.; Pickens, M. W.; Ter Haar, L. W.; Weller, R. R. In *Extended Linear Chain Compounds*; Miller, J. S., Ed.; Plenum Press: New York and London, 1983.
(27) Swank, D. D.; Landee C. P.; Willett, R. D. *Phys. Rev.* **1979**, *B20*, 2154.
(28) Keller, E. SCHAKAL 88: A Fortran Program for the Graphic Representation of Molecular and Crystallographic Models. University of Freiburg, Freiburg, Germany, 1988.